SYNTHESIS OF rGO/TiO_2 NANOWIRES DERIVED BY THERMAL OXIDATION OF TITANIUM AS A PHOTOCATALYST FOR Cr(VI) REDUCTION

SUBAGJA

UNIVERSITI SAINS MALAYSIA

2019

SYNTHESIS OF rGO/TiO_2 NANOWIRES DERIVED BY THERMAL OXIDATION OF TITANIUM AS A PHOTOCATALYST FOR Cr(VI) REDUCTION

by

SUBAGJA

Thesis submitted in fulfillment of the

requirements for the degree of

Master of Science

May 2019

ACKNOWLEDGEMENT

Alhamdulillah, all praise be to Allah for His grace and mercy in completing of my master study.

First of all, I would like to express my gratitude to my supervisor, Assoc. Prof. Dr. Zainovia Lockman for her knowledge, guidance, and encouragement throughout my study in USM. Thanks also to my advisor, Prof. Atsunori Matsuda from Toyohashi University of Technology (TUT), Japan.

Special acknowledgement to ASEAN University Network for Science and Engineering Education Development Network (AUN/SEED-Net), Japan International Cooperation Agency (JICA), and Research University Grant (USM-TUT Collaboration) for supporting my research and study here. I would like to thank to all AUN/SEED-Net executive and staff, especially Prof. Dr. Ueda Tamon, Ms. Wanichar, and Ms. Tong for their kind assistance.

I also would like to thank to the Dean of School of Materials and Mineral Resources Engineering (SMMRE) USM, Prof. Madya Ir. Dr. Syed Fuad Saiyid Hashim, Prof. Dr. Ahmad Fauzi Mohd Noor as a manager for AUN/SEED-Net students in USM, lecturers, staff, and technicians.

Special thanks to GEMs group members; Dr. Monna Rozana for all her help and supports, Dr. Mustafa Ali Azhar, Nurulhuda Bashirom, Chan, Izza, Afiq, Ain, Wani, Azlina. To all AUN/SEED-Net students; Bee, Pla, Hay mar, Han, Adriana, Trang, Kanchana, Thi, Tam, Zarni, Thet thet, Phyo, Sopheak, Ma zin, Han min, Piseth, Uyen, Trinh. Pak Syafrudin and Bu Aci for support, warmth, and great companion. To all post graduate students of SMMRE USM, thanks for everything.

To my parents (Toto and Turina), my sisters (Kurtati and Rustianti) for their endless love and support. Last but not least, to everyone who has contributed to the success of my master study, thank you.

Subagja

May, 2019

TABLE OF CONTENTS

LIST OF TABLES

LIST OF FIGURES

LIST OF ABBREVIATIONS

a.u.	Arbitrary Unit
ads	Adsorption
BSE	Backscattered Electrons
CB	Conduction Band
Cr(III)	Chromium(III)
Cr(VI)	Chromium(VI)
DC	Direct Current
DI	Deionized Water
EDTA	Ethylene Diamine Tetraacetic Acid
EDX	Energy Dispersive X-Ray
FESEM	Field Emission Scanning Electron Microscopy
FWHM	Full Width High Maximum
HRTEM	High Resolution Transmission Electron Microscopy
ISO	International Organization for Standardization
NHE	Normal Hydrogen Electrode
NWs	Nanowires
PDF	Powder Diffraction File
pH	Hydrogen potential
PL	Photoluminescence
SAED	Selected Area Electron Diffraction
SE	Secondary Electron
TEM	Transmission Electron Microscopy
TNWs	TiO_2 Nanowires
UV	Ultraviolet
UV-Vis	Ultraviolet-Visible Spectrophotometer

VB	Valence Band
XPS	X-Ray Photoelectron Spectroscopy
XRD	X-Ray Diffraction

LIST OF SYMBOLS

%	Percentage
°	Degree
°C	Degree Celcius
°C/min	Degree Celcius per minute
θ	Bragg angle
2θ	Diffraction angle
λ	Wavelength
ϕ_{BH}	Schottky barrier height
d_{BW}	Schottky barrier width
E_C	Conduction band energy
E_{FG1}	Fermi energy level of graphene before deposition
E_{FG2}	Fermi energy level of graphene after deposition
E_{FT1}	Fermi energy level of TiO_2 before deposition
E_{FT2}	Fermi energy level of TiO_2 after deposition
E_g	Bandgap energy
E_V	Valence band energy
e^-	Electrons
G	Gram
$OH^\bullet$	Hydroxyls radical
h^+	Holes
$h\upsilon$	Photon energy
Mg	Milligram
Min	Minute
mL	Millilitre

Mm	Millimeter
nm	Nanometer (10^{-9} m)
s	Second
T	Temperature
$Vo^{\bullet\bullet}$	Oxygen vacancies

SINTESIS DAWAINANO rGO/TiO_2 DIPEROLEHI DENGAN PENGOKSIDAAN TERMAL TITANIUM SEBAGAI FOTO-PEMANGKIN UNTUK PENURUNAN Cr(VI)

ABSTRAK

Dawai-nano TiO_2 (NWs) telah disintesis melalui pengoksidaan terma dengan pemangkin kalium hidroksida (KOH) dalam wap air. Terdapat dua langkah pemanasan yang dilakukan; i) pemendapan KOH dan ii) proses pengoksidaan. Kesan suhu pengoksidaan, masa, keadaan KOH, dan keadaan wap air telah diselidik dalam pembentukan dawai-nano. Ia menunjukkan bahawa dawai-nano boleh tumbuh pada kerajang titanium teroksida dengan KOH pada 550 – 750 ^oC dalam wap air. Dawai-nano terbentuk menjadi lebih panjang, tebal dan padat kerana peningkatan suhu pengoksidaan. Walau bagaimanapun, pada 750 ^oC, sebahagian dawai-nano bergabung dengan dawai-nano bersebelahan menyebabkan kepadatan kawasan berkurang. Purata panjang dan diameter sampel dawai-nano pada 750 ^oC yang teroksida adalah masing-masing 621 nm dan 73 nm. Oleh kerana proses pengoksidaan bergantung pada masa; panjang, diameter dan kepadatan kawasan dawai-nano telah meningkat apabila masa pengoksidaan lebih panjang. Kedua-dua KOH dan wap air adalah penting untuk pertumbuhan dawai-nano. Dari belauan sinar-X (XRD), spektroskopi Raman, resolusi tinggi mikroskopi electron transmisi (HR-TEM), spektroskopi fotoelektron sinar-X (XPS), dawai-nano terdiri daripada fasa rutile TiO_2 dan $K_2Ti_6O_{13}$ atau sebatian diperkaya-K. Mekanisma pertumbuhan dawai-nano melalui pengoksidaan terma dengan pemangkin KOH dalam wap air terdiri daripada pencecairan KOH, keutamaan penyerapan juzuk (Ti^{4+}, O^{2-}, OH^-) dalam titisan, penukleusan TiO_2 dalam titisan, “pembentukan selaput-K”, perencatan pertumbuhan sisi dan pertumbuhan paksi-c kerana “selaput sebatian-K” untuk pembentukan struktur dawai-nano. Pengurangan grafin oksida (rGO) dienapkan di atas TiO_2 NWs dengan kaedah pemendapan electroforesis (EPD). Kaedah ini dapat mengurangkan kumpulan yang mengandungi oksigen seperti yang disahkan oleh spektroskopi Raman dan XPS. Sampel

TiO_2 NWs dan rGO/TiO_2 NWs digunakan sebagai fotopemangkin untuk penurunan Cr(VI) di bawah cahaya UV dan cahaya nampak. Di bawah UV, sampel rGO/TiO_2 NWs menghasilkan 100% penurunan 10 mg mL^{-1} Cr(VI) dalam tempoh 30 min. Sedangkan sampel TiO_2 NWs menurunkan jumlah Cr(VI) yang sama dalam tempoh 60 min. Di bawah cahaya nampak, hanya sampel rGO/TiO_2 NWs melakukan penurunan 100% Cr(VI) dalam masa 60 min, manakala tidak bagi sampel TiO_2 NWs. Sekiranya rGO/TiO_2 NWs disinari di bawah cahaya nampak, elektron terhasil cahaya dalam rGO boleh dipindahkan ke TiO_2 NWs dan penurunan Cr(VI) berlaku. Sementara di bawah UV, pembentukan pasangan elektron-lubang berlaku pada TiO_2 NW kerana tenaga foton yang lebih tinggi daripada jurang jalurnya. Fotojana elektron boleh dipindahkan secara spontan dari TiO_2 NWs ke rGO untuk menurunkan Cr(VI). Pemendapan rGO pada TiO_2 NWs mewujudkan medan elektrik terbina dalam TiO_2 NWs yang boleh menyekat penggabungan semula pasangan elektron-lubang mengakibatkan peningkatan prestasi fotopenurunan Cr(VI).

SYNTHESIS OF rGO/TiO_2 NANOWIRES DERIVED BY THERMAL OXIDATION OF TITANIUM AS A PHOTOCATALYST FOR Cr(VI) REDUCTION

ABSTRACT

TiO_2 nanowires (NWs) were synthesised by thermal oxidation with potassium hydroxide (KOH) catalyst in water vapour. There were two heating steps required in its synthesis; i) KOH deposition, ii) oxidation process. The effect of oxidation temperature, time, KOH presence, and water vapour presence were investigated on the formation of nanowires. It shows that nanowires can grow on oxidised titanium foil with KOH at 550 - 750°C in water vapour. The nanowires formed became longer, thicker, and denser as oxidation temperature increased. However, at 750°C, some of nanowires merged with adjacent nanowires resulted in lower areal density. The average length and diameter of nanowire at 750°C oxidised sample are 621 nm and 73 nm respectively. As oxidation is time dependent process, the length, diameter, and areal density of nanowire were increased as the oxidation time was longer. Both KOH and water vapour were essential for the growth of nanowire. From X-ray diffraction (XRD), Raman spectroscopy, High Resolution Transmission Electron Microscopy (HR-TEM), X-ray Photoelectron Spectroscopy (XPS) results, the nanowires formed consist of rutile TiO_2 and $K_2Ti_6O_{13}$ phase or K-rich compound. Growth mechanism of nanowire via thermal oxidation with KOH catalyst in water vapour consists of KOH liquefaction, preferential absorption of constituents (Ti^{4+}, O^{2-}, OH^-) in the droplets, nucleation of TiO_2 in the droplets, formation of "K-compound-shell", lateral growth inhibition and c-axis growth due to "K-compound-shell" to form nanowire structure. Reduced graphene oxide (rGO) was deposited onto TiO_2 NWs sample by electrophoretic deposition (EPD) method. This method can reduce oxygen-containing group as confirmed by Raman spectroscopy, and XPS results. TiO_2 NWs and rGO/TiO_2 NWs samples were used as photocatalyst for Cr(VI) reduction under UV and visible light. Under UV, rGO/TiO_2 NWs

sample performed 100% reduction of 10 mg mL^{-1} Cr(VI) within 30 minutes. Whereas TiO_2 NWs sample reduced the same amount of Cr(VI) within 60 minutes. Under visible light, it was only rGO/TiO_2 NWs sample that performed 100% reduction of Cr(VI) within 60 minutes, while TiO_2 NWs sample did not. In case of rGO/TiO_2 NWs irradiated under visible light, photogenerated electrons in rGO can be transferred to TiO_2 NWs and Cr(VI) reduction occurred. While under UV, electron – hole pairs formation was happened in TiO_2 NWs due to higher photon energy than its band gap. Photogenerated electrons can be transferred spontaneously from TiO_2 NWs to rGO to reduce Cr(VI). Depositing rGO on TiO_2 NWs creates built-in electric field in TiO_2 NWs that can suppress recombination of electron – hole pairs resulted in the enhancement of photoreduction of Cr(VI) performance.

CHAPTER ONE

INTRODUCTION

1.1 Background

World population has now reached 7.6 billion and increases about 1% every year (UN, 2017). This translates to increasing demand for food, energy, transportations, housings, goods, and the other necessities which then lead to the rise of industrial activities, agriculture and power generation. As the population increases even more, there is an increase in the amount of pressure put on the industrial sector. Goods are being produced by manufacturers at a higher rate as to satisfy demand and this can have a negative impact on the environment if wastes from such anthropogenic activities are not being treated properly. Discharged of effluent containing toxic chemicals and substances from industrial establishment to water bodies can cause harm to human and animals.

Among various chemical being released to the surface water from anthropogenic sources, heavy metals are perhaps one of the most dangerous. The excess amount of heavy metals can harm aquatic life, and accumulated in humans via biomagnifications. Heavy metals are defined as a block of all metals with high densities in periodic table in groups 3 to 16 that are in periods 4 and greater (Hawkes, 1997). As can be seen in Table 1.1, they are classified as essential, possibly essential, and non-essential according to the characteristics of health effects (Goyer et al., 2004). The first has an important role in biochemical and physiological function in plants, animals, or humans. The second is non essential but possibly has beneficial health effect. Meanwhile, the last category has no biochemical functions or even toxic for humans, and other living organisms. According to International Agency for Research on Cancer (IARC), arsenic, cadmium, and chromium(VI) are classified in group 1 which means carcinogenic to humans (IARC, 2018). Several studies have been done to test the carcinogenity of these elements in animal and human cells. The results are concluded that there is adequate evidence that the elements are carcinogen(Sun et al., 2014)

(García-Esquinas et al., 2014) (Wu et al., 2016). On the other hand, lead and mercury are classified in group 2A and 3 which the carcinogenity is still controversial (IARC, 2018). However, excess amount of lead and mercury in human body can cause serious health issues like nerve related diseases (Mason et al., 2014) (Gibb and O'Leary, 2014) leading to behavior changes which is detrimental in children growth and social behavior.

Table 1. 1 Classification of heavy metals based on characteristics of health effects (Goyer et al., 2004)

Essential Heavy Metals	**Non-Essential Heavy Metals with Possible beneficial health effect**	**Non-Essential Heavy Metals**
Cobalt	Boron	Arsenic
Chromium(III)	Nickel	Cadmium
Copper	Silicon	Chromium(VI)
Iron	Vanadium	Lead
Manganese		Mercury
Molybdenum		
Selenium		
Zinc		

Heavy metals contamination in water bodies (river, ground water, lake) must therefore be avoided as even in small concentration, accumulation is inevitable especially in aquatic life. Furthermore, if heavy metal polluted water is used for irrigation, accumulation of heavy metal in agricultural soils can lead to absorption by the plants. When the crops are being consumed by human, the ions can be transferred and accumulate which then can bring negative health effect (Chen et al., 2018). Moreover, aquatic life which live in water bodies such as fish, mussels, and oysters also can be contaminated by heavy metals (Rajeshkumar et al., 2018). Consuming them would lead to bioaccumulation in human.

As mentioned above, chromium(VI) is one of the heavy metals that can cause cancer to human. According to WHO standards, the permissible limit of total chromium in drinking water is not more than 0.05 mg/L (WHO, 2011). Chromium(VI) which also known as hexavalent chromium is far more toxic and less stable than chromium(III). Cr(VI) compounds are however very important. They are being widely used in industry as textile dyes, pigments, leather tanning and paints. Cr(VI) compounds are also known to have excellent corrosion resistance properties and hence has been used as corrosion inhibitors. Chrome metal plating or stainless-steel also uses Cr(VI) compounds in a large quantity. Unless properly treated, the discharge of effluents from these industries to the environment is considered as one of the major factor of Cr(VI) pollution in the world.

Table 1.2 shows Cr(VI) pollution in surface water and ground water from several countries in the world. Gao and Xia in 2011 reported the excessive amount of Cr(VI) in the Nanpan river of China was due to untreated chromium waste from nearby chemical industry. This accident caused fatality of some people and cattle from nearby village. The second highest concentration of Cr(VI) on the list was found in Italy with not less than 17.97 mg/L in the highly polluted Sarno river. This was caused by lacking of respect of the law, and anthropogenic sources (Basile et al., 2015). In 2010, Cikijing river in Indonesia and estuaries in Pulau Pinang Malaysia have been reported to have exceeded in the standard concentration of Cr(VI) (Roosmini et al., 2010), (Ismail et al., 2016). Furthermore in African continent, a high level Cr(VI) concentration was found at Léré lake in Chad (Mahamat et al., 2017). Meanwhile, for ground water pollution with high content of Cr(VI), it was found in Sukinda Chromite mine area in India (Naz et al., 2016) and California in United States (Izbicki and Groover, 2018).

Table 1.2 Cr(VI) pollution in several countries in the world

No.	Year	Concentration (mg/L)	Sites	Water Pollution	Countries	References
1	2017	0.15 - 2.5	MW-178S/D; MW-208/209S California	Ground Water	United States	(Izbicki and Groover, 2018)
2	2016	0.03 - 0.50	Léré lake	Surface Water	Chad	(Mahamat et al., 2017)
3	2014	1.8 - 17.97	Sarno river	Surface Water	Italy	(Basile et al., 2015)
4	2013	0.0214 – 0.1152	Sukinda Chromite Mine	Ground Water	India	(Naz et al., 2016)
5	2011	100	Nanpan river	Surface Water	China	(Gao and Xia, 2011)
6	2010	0.015 - 3.56	Cikijing river	Surface Water	Indonesia	(Roosmini et al., 2010)
7	2010	0.167	Pulau Pinang	Surface Water	Malaysia	(Ismail et al., 2016)

Several treatment technologies have been published to control Cr(VI) pollution in wastewater from industrial sector. In general, they are categorized as chemical precipitation (Kim et al., 2016), adsorption (Fang et al., 2018), filtration (Choudhury et al., 2018), electrodialysis (Chang et al., 2015), and semiconductor photocatalysis (Bashirom et al., 2018). All of them have advantages and disadvantages in operational, separation selectivity, by-product, energy consumption, process duration, applications, and costs. Among them, semiconductor photocatalysis is seen as the most promising as the process can treat even the smallest concentration of Cr(VI). Semiconductor photocatalysis technology relies on the electrons from the semiconductor to reduce Cr(VI) to Cr(III). As seen from Table 1.1, Cr(III) is not harmful to human and hence reduction of Cr(VI) to Cr(III) can be considered as an effective approach in reducing Cr(VI) from industry effluent. Moreover, reduction via photocatalayst is seen to be rather simple compared to other methods with low operational cost.

Semiconductor photocatalysis is a process to accelerate or initiate chemical reaction (oxidation or reduction) in the presence of semiconductor (photocatalyst) that absorbs light energy (UV, visible, or infrared radiation) (Braslavsky et al., 2009). Semiconductor photocatalysis utilize semiconductor as a substance (photocatalyst) that can generate electron - hole pairs under light irradiation with the energy higher than its band gap. The photogenerated electrons in semiconductor are used to reduce Cr(VI) to Cr(III) in industrial wastewater. Various semiconductors have been reported as photocatalyst for Cr(VI) reduction such as TiO_2 (Bashirom et al., 2018), ZnO (Wang and Ni, 2018), Fe_2O_3(Gao et al., 2018), and CuO (Li et al., 2017). Among all those listed, conventional photocatalysts, TiO_2 is chosen for Cr(VI) reduction application as the material can generate high quantum yields, chemically stable, insoluble under most conditions, photostable, non-toxic, and inexpensive (Chen et al., 2000).

In this research, TiO_2 nanowires were synthesised on titanium foil. TiO_2 nanowire is 1-D nanostructured material which has two dimensions (a – b planes/axes) in nanoscale (1 - 100 nm) and one dimension (c plane/axis) not in nanoscale (ISO, 2015). Nanostructured materials have improved properties than their bulk counterpart due to much higher surface area, high volume to surface ratio and high surface energy. Surface atoms have distinctively different properties than atoms in the bulk due to incomplete bonding the atoms have. This makes them more reactive and therefore is expected to have much improved photocatalytic performance of TiO_2.

There are several routes to synthesis TiO_2 nanowires such as hydrothermal (Mokhtar et al., 2018), thermal evaporation (Shang et al., 2012), liquid phase deposition with porous alumina template (Attar and Hassani, 2015). However, these methods have drawbacks like time consuming, required special chemicals, high temperature, and the distribution of nanowires on the substrate is rather poor. On the other hand, thermal oxidation technique is simple, fast, scalable, and able to obtain dense nanowires formation (Cheung et al., 2007).

Oxidation of metal can be defined as reaction between metal and oxidant (usually oxygen) to form oxide scale on metal surface. When conducted at high temperature the growth of the oxide increases rapidly due to the growth of the oxide film. Oxidation for nanowires formation can be done at elevated temperature under certain conditions. In this work, titanium was oxidised as to produce TiO_2 nanowires on the surface.

Nevertheless, as will be described later the oxidation process for nanowires formation is not as straight forward as oxidation often resulted in compact oxide film on titanium (Kofstad, 1958). Therefore, catalysts are required as to confine the growth of the metal oxide in c-direction hence elongated nanostructure; nanowire is formed. This can occur due to growth confinement by the catalysts.

KOH was selected as catalyst as it is abundant, not toxic and rather cheap. KOH assisted oxidation process is also seen as a simple, relatively low oxidation temperature, and potential for large scale production. Oxidised titanium was characterized using Field Emission Scanning Electron Microscopy (FESEM), High-Resolution Transmission Electron Microscopy (HRTEM), X-ray Diffractometer (XRD), Raman Spectroscopy, X-ray Photoelectron Spectroscopy (XPS), and Photoluminescence (PL). The reduction performance of the TiO_2 nanowires can be assessed by UV-Visible Spectrophotometry (UV-Vis).

TiO_2 has two major drawbacks: wide bandgap, and high recombination electron – hole pairs. The wide bandgap of TiO_2 (3.2 eV for anatase, and 3.0 eV for rutile) requires high energy photons (UV light) to generate electron – hole pairs. The high recombination of TiO_2 is commonly caused by surface defects (oxygen vacancies) in n-type semiconductor which can act like recombination center (Schneider et al., 2014). It can reduce its photocatalytic performance. The solution for these issues is by combining TiO_2 with graphene. Graphene is a single layer of carbon atoms which has hexagonal honeycomb lattice. Unlike another method to lower the bandgap of TiO_2 by doping with impurities,

modification of TiO_2 with graphene does not create new recombination centers (Tang et al., 2018). Depositing a zero bandgap graphene on TiO_2 enables the absorption of visible light to generate photo-induced electrons. In addition, the coupling results in built-in electric field in TiO_2 which affects to the fast charge carriers transfer between graphene and TiO_2 (Ou, 2015). This can effectively suppress the recombination of the photo-generated electron – hole pairs in TiO_2.

Formation of TiO_2 - graphene nanocomposite can be done in various ways. Hydrothermal is the most used method to fabricate TiO_2 - graphene nanocomposite (Shen et al., 2011) (Liu et al., 2016a) (Wu et al., 2015). However, this method requires long duration, and special chemicals which may influence the properties of TiO_2. In this work, graphene was obtained from chemical reduction of graphene oxide (GO) using vitamin C at 95 °C as known as reduced graphene oxide (rGO) which properties are almost similar with pristine graphene (Fernández-Merino et al., 2010). This reduction technique was selected in this work because of cost-effective, scalable, and easy for deposition onto other material. The deposition of rGO on as-synthesised TiO_2 nanowires was done by electrophoretic deposition (EPD) method. EPD is a common technique to deposit suspended particles onto the substrate (electrodes) by electric field. By this route, the fabrication of rGO/TiO_2 nanowires can be facile, effective, and potential for large-scale production.

1.2 Problem statements

This project was on the formation of TiO_2 nanowires on titanium foil via thermal oxidation of titanium. The synthesis of TiO_2 nanowires by thermal oxidation was probably first published by Motte et al. in 1976. They obtained whiskers after oxidising pure titanium plate at 650 °C for 120 hours in water vapour atmosphere. However, this method is time consuming and not practically accepted. A process which is quick and economical is desired.

Peng and Chen in 2004 have successfully fabricated TiO_2 nanoribbons by oxidation done in two conditions (Peng and Chen, 2004). First, they oxidised titanium plate at 850 °C

for 1.5 hours in very low concentration of oxygen gas (1 sccm). Second, they oxidised titanium plate in acetone vapour with the same oxidation temperature and duration. They found that low oxygen concentration during oxidation of titanium played a substantial role for TiO_2 nanowires formation. A similar technique was also done by Daothong et al. (Daothong et al., 2007) and Huo et al. (Huo et al., 2009) several years after Peng and Chen published work. Despite the success, the nanowires formed have amorphous carbon shell covering the TiO_2 core. Therefore, post annealing is needed to remove this shell. The easiest method to synthesis TiO_2 nanowires by thermal oxidation was done with Lee in 2016 (Lee, 2016). Lee heated TiO powders in air for 2 hours to obtain nanowire structures on the substrate. Nevertheless, the oxidation temperature is considered very high (1000 °C) and the product is different than oxide nanowires on titanium foil.

The application of catalyst in whiskers (or nanowires) formation was introduced by Wagner and Ellis for the formation of silicon (Si) whiskers with Au catalyst via Vapour Liquid Solid (VLS) mechanism (Wagner and Ellis, 1964). According to Wagner and Ellis, liquid droplets are required to confine silicon growth to form the whiskers. Therefore, first, they made liquid droplets on a substrate from metal catalyst at high temperature. The liquid droplets were preferential sites for adsorbing vapour components (in their case silicon vapour). As silicon diffused in the metal droplets, a liquid alloy was formed and with constant exposure to silicon vapour, the droplet was supersaturated resulting in precipitation of Si at the liquid–solid interface. Si wires will grow from underneath the droplet and continued to elongate (in c-axis) as long as the vapour components were supplied. Because vapors (silicon precursor), liquid (alloy catalyst at high temperature), and solid (precipitated Si whisker) phases are involved, the process is termed as VLS process. The final whisker formed would have cap at the top if the Au was not consumed during the process.

Arcadipane et al. have implemented the same method to synthesis TiO_2 nanowires by depositing Au catalyst on thin layer of titanium and heated at 700 °C for 4 hours in low concentration of oxygen (0.1 L/min) mixed with argon gas (1.5 L/min) (Arcadipane et al.,

2016). Oxidation is a process that relies on the diffusion of Ti^{4+} ions from the substrate upwards. There is no vapour of Ti^{4+} being exposed to the catalyst and hence VLS mechanism for oxide nanowires formed by thermal oxidation is not exactly correct. By using Au as catalysts, the TiO_2 nanowires formed are relatively short with low areal density. On the other hand, another researchers have successfully fabricated longer TiO_2 nanowires with potassium catalyst in humid atmosphere (Cheung et al., 2007) (Lee, 2014). Cheung et al. used titanium foil as a substrate and potassium fluoride (KF) as a catalyst in their research while Lee used thin film of titanium and KOH as a substrate and catalyst respectively. Both researches obtained long nanowires (10 μm) with high areal density (good coverage on the titanium substrate). Moreover, the oxidation temperature for nanowires formation is lower than previous researches (450 - 650 °C). VLS was proposed as the growth mechanism of the nanowires in their report. It is however believed that VLS is not appropriate as titanium has high vapour pressure that at such low temperature, it would not have formed. Moreover, from the microscopy observation, no catalyst cap was present at the tip of nanowires. The mechanism on TiO_2 nanowires growth by oxidation is still vague and requires further clarification thus this work was done to investigate further on this matter.

In this work, TiO_2 nanowires were synthesised by thermal oxidation with KOH catalyst using titanium foils as a substrate in water vapour atmosphere. It is of interest to investigate the influence of oxidation parameters to nanowires formation and hence to decide on the growth mechanism of the nanowires on titanium. The main aim was to produce nanowires on titanium at as low temperature as possible and as fast as possible; in effort to reduce energy and time during nanomaterials processing and fabrication.

As mentioned, the nanowires formed were intended to be used as photocatalysts for Cr(VI) reduction. Despite the importance in removing Cr(VI) from wastewater, there is a limited amount of publications on the subject of reduction of Cr(VI) by TiO_2 as photocatalysts. Moreover, as to date there is no published works on the use of thermally oxidized TiO_2 nanowires for Cr(VI) reduction. Therefore in this work, reduction

of Cr(VI) on TiO_2 nanowires were performed and the performance of the nanowires was assessed with main aim as to have a complete reduction at short time.

Reduction of Cr(VI) on photocatalyst can be best done under sunlight as oppose to artificial light as this translates to a more robust water treatment facility. However, as stated before, TiO_2 is a wide gap semiconductor and hence it can only be activated under UV light. Sunlight has only 5% of UV light. Therefore photoreduction of Cr(VI) by TiO_2 under sunlight can be expected to be rather slow. By combining graphene with TiO_2 it is expected to enhance absorption of visible light and to suppress recombination electron – hole pairs on the graphene/TiO_2 photocatalyst. As a result, it can perform optimum photoreduction of Cr(VI) under sunlight or visible light.

There are many publications about rGO/TiO_2 nanocomposite (TiO_2 mostly in a form of particles or nanoparticles) available for photocatalyst applications (Wang, 2014) (Žerjav, 2017) (Giovannetti, 2017). Nevertheless, there are not much been done on the fabrication of rGO/TiO_2 nanowires by chemical reduction and EPD. Therefore, it was challenging to investigate the reduction and deposition process as well as on assessing the performance in reducing Cr(VI).

1.3 Objectives of study

The main objectives of this research are:

1. To study the effect of oxidation temperature, time, KOH presence, and water vapour presence in the formation of TiO_2 nanowires by thermal oxidation.
2. To elucidate the growth mechanism of TiO_2 nanowires in the presence of KOH catalyst.
3. To fabricate rGO/TiO_2 nanowires composite by combined method (chemical reduction and EPD).

4. To assess and to compare the performance of TiO_2 nanowires, and rGO/TiO_2 nanowires composite as photocatalyst for Cr(VI) reduction under UV and visible light.

1.4 Scope of research

The scope of this research mainly covers the synthesis TiO_2 nanowires by thermal oxidation with KOH catalyst, fabrication rGO/TiO_2 nanowires by combined method (chemical reduction and EPD), and photocatalysis of Cr(VI) reduction. The oxidation parameters used are oxidation temperature, oxidation time, KOH and water vapour. The synthesised TiO_2 nanowires and rGO/TiO_2 nanowires samples were characterized by Field Emission Scanning Electron Microscopy (FESEM), X-ray Diffraction (XRD), Raman Spectroscopy, High - Resolution Transmission Electron Microscopy (HRTEM), Energy Dispersive X-ray Spectroscopy (EDX), Selected Area Electron Diffraction (SAED), X-ray Photoelectron Spectroscopy (XPS), and Photoluminescence (PL). The growth mechanism of TiO_2 nanowires was discussed as well as photocatalytic mechanism of Cr(VI) reduction by TiO_2 nanowires and rGO/TiO_2 nanowires. The kinetic study of Cr(VI) reduction was also studied in this research.

1.5 Thesis outline

This thesis consists of five chapters. Chapter one explains about background of this reseach, the important of this research, drawbacks of previous researches, reasons of selection the chosen method, objectives of this research, scope of this research, and outline of this thesis. Chapter two contains literature review and fundamental theory about titanium, TiO_2, oxidation of titanium, synthesis TiO_2 nanowires by thermal oxidation, growth mechanism of TiO_2 nanowires with catalyst, graphene and its properties, EPD method, and photocatalysis of Cr(VI) reduction. In chapter three, methodology used in this research is

explained in details. Materials, chemicals, and equipments used in this research were explained including characterizations techniques and photocatalysis experiment. Furthermore, in chapter four, all results and observations from the experiment are shown and discussed including the effect of oxidation parameters in the formation of nanowires, growth mechanism of nanowires formed, and photocatalysis mechanism and kinetic of Cr(VI) reduction. Last but not least, in chapter five contains conclusions of this research and suggestions for the next research.

CHAPTER TWO

LITERATURE REVIEW

2.1 Introduction

This chapter contains of summary of knowledge, theoretical base, and previous researches used as a reference in this work. It is started with description of titanium, titanium oxide, their properties, and applications. Next, nanomaterial definition, classification, properties, and its synthesis methods are explained briefly. Oxidation of titanium and several influence factors in the process are also presented in the next section. Previous researches in synthesising TiO_2 nanowires by thermal oxidation are reviewed as a comparison including growth mechanism of the nanowire with catalyst. As graphene was also used in this research, the basic knowledge of this material, synthesis process, and deposition method by EPD are explained in this chapter. Photocatalysis process in reducing Cr(VI) is presented in the last part.

2.2 Titanium

Titanium (Ti) is a transitional metal with atomic number 22 in group 4 periodic table. It is widely known for its application in aircraft, aero-engines, biomedical devices, and chemical processing equipments due to its high strength, low density, creep resistance in high temperature, and corrosion resistant. In earth's crust, the amount of titanium is about 0.6% and ranked in the fouth most abundant metal after aluminium, iron, and magnesium (Lutjering and Williams, 2007). However, the production of titanium is rather difficult as the metal can easly react with oxygen and nitrogen. This might cause the relatively high cost of titanium and hinder for wider use.

Table 2.1 shows the basic characteristics of titanium and other metals. As seen, titanium has the best characteristic in terms of high melting point, low density, and very high

corrosion resistant compared to iron, nickel, and aluminium. In room temperature, titanium exists in α-phase with hexagonal close packed (HCP) crystal structure having lattice parameters of a = 0.295 nm and c = 0.468 nm giving a c/a ratio of 1.587. It will transform to body centered cubic (BCC) structure (β-phase) with a lattice parameter of 0.332 nm at high temperature (882 °C). However, β-phase titanium can exist in room temperature by alloying with high concentrations of β stabilizing elements.

Table 2. 1 Some of the important characteristics of titanium as compared to other metals (Lütjering and Williams, 2007)

	Ti	Fe	Ni	Al
Melting Temperature (°C)	1670	1538	1455	660
Allotropic Transformation (°C)	$\beta \xrightarrow{882} \alpha$	$\gamma \xrightarrow{912} \alpha$	-	-
Crystal Structure	bcc → hex	fcc → bcc	fcc	fcc
Room Temperature E (GPa)	115	215	200	72
Yield Stress Level (MPa)	1000	1000	1000	500
Density (g/cm^3)	4.5	7.9	8.9	2.7
Comparative Corrosion Resistance	Very High	Low	Medium	High
Comparative Reactivity with Oxygen	Very High	Low	Low	High
Comparative Price of Metal	Very High	Low	High	Medium

2.3 Titanium Dioxide

Titanium dioxide (TiO_2) is an n-type semiconductor metal oxide. It is widely used as white pigment (in paint, or cosmetics), photocatalyst (for pollutant degradation, water splitting), gas sensor, solar cells, corrosion-protective coating, optical coating due to its excellent properties such as chemical stability, photostability, non-toxic, insoluble for most solvent, and highly photoactive. The properties of TiO_2 is closely related to its crystal structure. It has three main different crystal structures; rutile, anatase, and brookite. However, only rutile and anatase have gain the most research interest for many applications. Both have tetragonal structure with lattice parameters a=b= 4.584Å, c= 2.953Å for rutile; and a=b= 3.782Å, c= 9.502Å for anatase. Their bulk unit cells are shown in Figure 2.1.

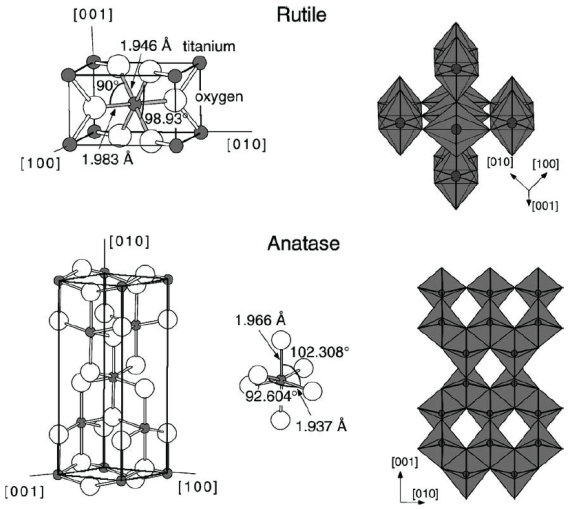

Figure 2. 1 Bulk unit cells of rutile and anatase (Diebold, 2003)

Figure 2.2 shows the electronic density of states (DOS) for rutile and anatase. The valence band edge for both phases is dominated by O 2p, and the conduction band edge is formed from Ti 3d. The excess electrons in these phases will be centered on the d states of cations, while holes are centered on 2p states of oxygen. The energy gap between conduction band and valence band for rutile and anatase are 3.0 eV and 3.2 eV respectively. Measured band gap of TiO_2 is 3.24 eV and for nanostructured TiO_2 the band gap is reduced to 3.09 eV (Khan et al., 2015).

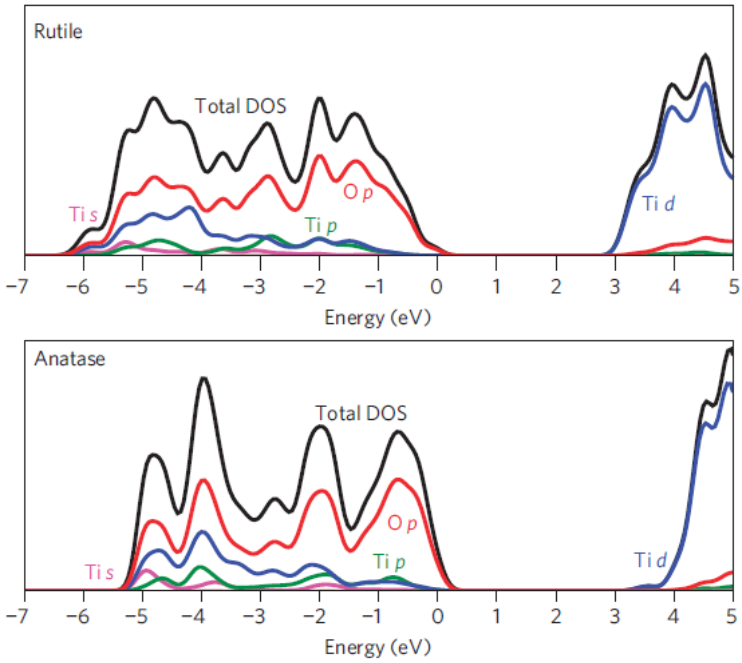

Figure 2. 2 Density of states (DOS) of rutile and anatase (Scanlon et al., 2013)

2.4 Oxidation of titanium

Oxidation is a process of loss of electron or an increasing oxidation state by atoms, molecules, or ions. Oxidation of metal reactions are often associated with the formation of oxides on metal surface. In the case of titanium, oxidation at ambient condition is difficult to occur as titanium has a very high corrosion resistance properties. Moreover, it can accommodate up tp 33 at% oxygen before forming a stable oxide (Massalski et al., 2001). However, several studies have been reported on oxidation of titanium at low and high temperatures with various oxidation parameters (Kofstad et al., 1958) (Gemelli and Camargo, 2007) (Kumar et al., 2010).

In this work, oxidation of titanium is directed to form titanium oxide scale with nanowire structure. This section is also focused on oxidation of titanium at temperature from 500 to 800 °C in air and water vapour atmosphere. However, other oxidation conditions will be explained in the next section.

2.2.1 Thermodynamic of titanium oxide formation

Thermodynamic study of titanium oxide formation is needed to determine whether an oxide can be formed or not at particular temperature and pressure. Figure 2.3 shows Ellingham/Richardson diagram of several metal oxides. The diagram consists of Gibbs free energy graph in the box for various metal oxides as a function of temperature and the corresponding dissociation pressure of the oxides. The Gibbs free energy change (ΔG) is defined as the driving energy for metal and oxygen to react with. Titanium oxide will only form if the partial oxygen pressure (pO_2) is higher than dissociation pressure of titanium oxide. In Ellingham/Richardson diagram, Gibbs free energy graph for titanium oxide is marked with yellow line, while dissociation pressure of titanium oxide at particular temperature is intersection between green dot line and pO_2 line. Therefore, if the oxidation of titanium is conducted these particular temperatures in ambient oxygen pressure, then titanium oxide will likely to form.

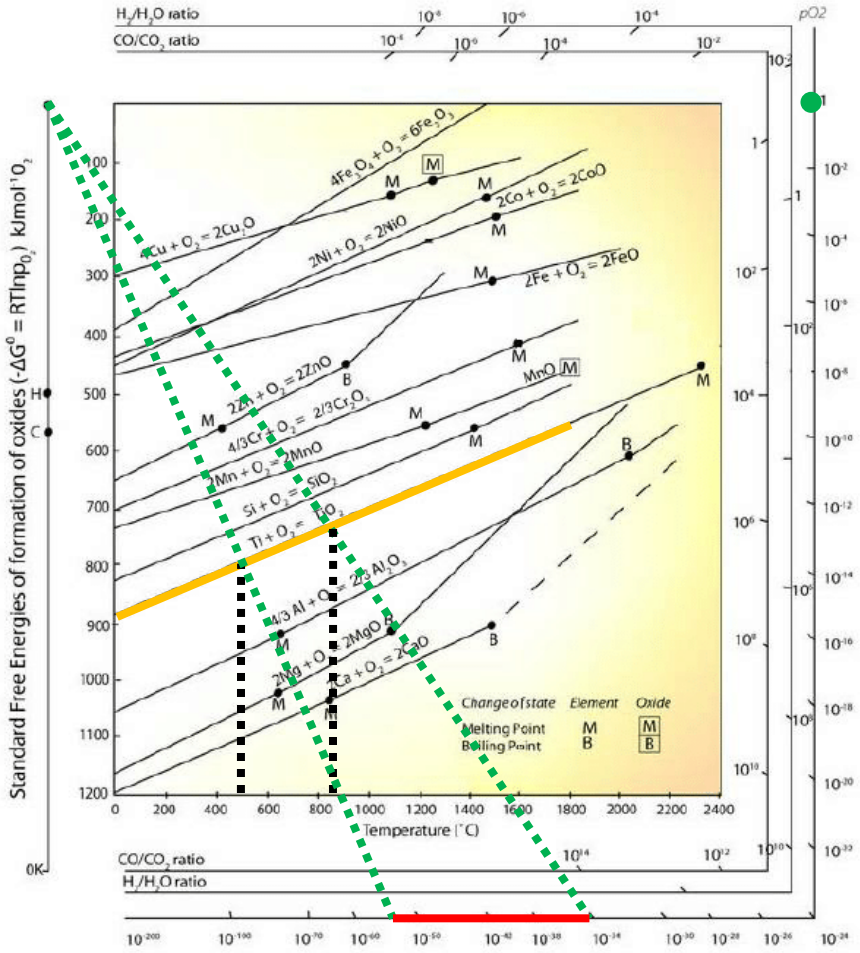

Figure 2. 3 Ellingham/Richardson diagram (Glazoff et al., 2015)

2.2.2 Mechanism of titanium oxidation

The process of titanium oxidation starts by chemisorption of oxygen (McCafferty, 2010) on the surface of titanium as expressed in equation 2.1. The oxygen ions (O^{2-}) on the surface of titanium will create negatively charged surface. At elevated temperature, titanium will be oxidised to become Ti^{4+} (equation 2.2) and diffuse out due to Coulombic attraction force and react with the O^{2-}.

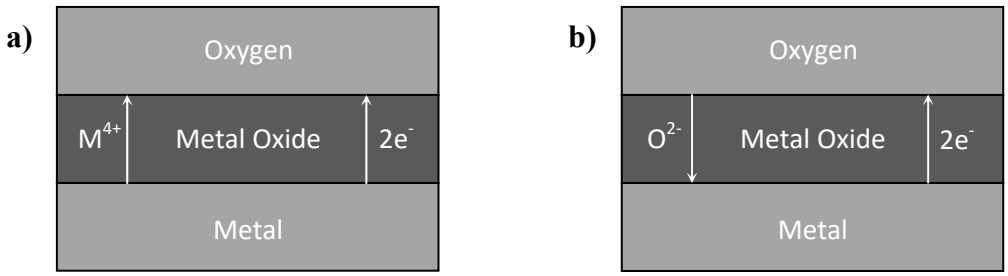

Figure 2. 4 Diffusion process in oxidation of metals at elevated temperature; a) Cations diffusion; b) Anions diffusion.

$$O_2 + 4e^- \rightarrow 2O^{2-} \quad (2.1)$$

$$Ti \rightarrow Ti^{4+} + 4e^- \quad (2.2)$$

$$Ti^{4+} + 2O^{2-} \rightarrow TiO_2 \quad (2.3)$$

Ti^{4+} and O^{2-} reaction results in titanium oxide layer (equation 2.3). Growth of the TiO_2 layer can only occur when the metal foil is heated up. As suggested by Wagner, oxidation of metal involves diffusion of ions and electrons (Wagner, 1938). Oxide scale is formed due to outward diffusion of metal cations and inward diffusion of oxygen anions (Figure 2.4 (a-b)). For the case of TiO_2 which is n-type anion-defective oxide, O^{2-} can diffuse faster than Ti^{4+} in the oxide layer through oxygen vacancies (Lutjering and Williams, 2007) (Galerie et al., 2001). This mechanism can indicate the formation of titanium oxide is in the metal/oxide interface or in the oxide scale.

2.2.3 Oxidation of titanium at 500 – 800 °C in air

There are many different results from published reports about oxidation of titanium at temperatures between 500 – 800 °C in air. Kumar et al reported that oxidation of titanium at 500 °C formed TiO and α-phase titanium, TiO and rutile TiO_2 at 650 °C, and completely rutile TiO_2 at 800 °C (Kumar et al., 2010). Gamelli and Camargo observed the formation of anatase and rutile TiO_2 at temperatures from 457 °C to 718 °C, and only rutile phase present at temperature above 718 °C (Gemelli and Camargo, 2007). Hickmann and Gulbransen

reported that only rutile phase formed on titanium after oxidation at 300 – 700 °C in air (Hickman and Gulbransen, 1948). Flower and Swann who carried out in-situ study of titanium oxidation observed rutile TiO_2 layer after oxidation at 450 – 850 °C (Flower and Swann, 1974). However, most of the reports agree that only rutile TiO_2 exist in the oxide after oxidation of titanium above 700 °C.

Oxidation rate of titanium at 500 – 800 °C in oxygen obeys parabolic rate law (Kofstad et al., 1958). This indicates that diffusion through the scale is the rate-determining process. Therefore, the thickness of the oxide can be expressed by equation 2.4. As *k*' value is constant, then for a given temperature the oxide thickens as oxidation time goes longer. Oxide scale also becomes thicker as oxidation temperature increased according to the report from Kofstad. However, several studies reported that dissolution of oxygen in the titanium also take place at the same time during oxide formation (Birks et al., 2006).

$$x^2 = 2k't \tag{2.4}$$

Where : x is the thickness of the oxide

t is the oxidation time

$k' = D_{VM} V_{OX} (C_{VM}'' - C_{VM}')$

D_{VM} is the diffusion coefficient for cation vacancies;

V_{OX} is the molar volume of the oxide;

C_{VM}'' is the vacancy concentrations at the scale – gas interfaces

C_{VM}' is the vacancy concentrations at the scale – metal interfaces

2.2.4 Oxidation of titanium at 500 – 800 °C in water vapour

Oxidation of Ti can be done in water vapour environment. It is well-known that oxidation rate in water vapour is faster than in oxygen. Wouters et al reported that mass gained was increased about three times in 20 mbar H_2O as compared with the rate in 20 mbar O_2 (Wouters et al., 1997). Wouters et al proposed that the faster rate of oxidation in water vapour was due to the incorporation of OH^- in the lattice. The faster diffusion is associated with the smaller size of OH^- than O^{2-}. In addition, Galerie et al suggested that interstitial proton defects ($H_i^{\bullet}$) may take into account in transportation of OH^- within the oxide (Galerie et al., 2001).

Several reports about oxidation of titanium at temperatures 650 – 850 °C in water vapour reveal that oxide formed is only rutile (Motte et al., 1976) (Wouters et al., 1997). There was no change in the conductivity of the oxide which remained n-type (Wouters et al., 1997). Both studies also discover the rate of oxidation of titanium in water vapour obey parabolic rate law.

2.3 Nanomaterial

Nanomaterial is defined as a material with any external dimension in the nanoscale or having internal structure or surface structure in the nanoscale (ISO, 2015). Nanoscale is a length range from 1 to 100 nm. Nanostructures include nanoparticles, nanowires, nanotubes, and thin films which have at least one dimension in nanoscale. The properties of nanomaterials can be significantly different than materials with the same chemical composition in the bulk form due to *size effects phenomena*. For instance, melting point of gold (Au) in the bulk form is 1,064 °C, but the melting point of gold in nanoparticle is decreased down to 925 °C, since higher surface energy of gold in nanoparticle size play a significant role in thermal stability.

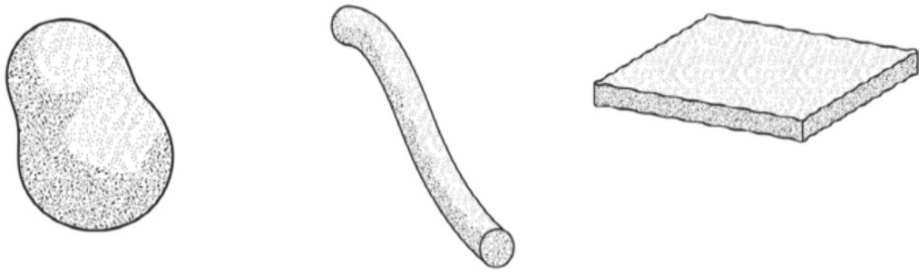

Figure 2. 5 Types of Nanostructure; (left to right) nanoparticle (three dimensions in nanoscale), nanowire (two dimensions in nanoscale), thin film (one dimension in nanoscale)

Nanostructured metal oxides like TiO_2 nanowires or nanotubes have gained its popularity in many applications such as battery (Liang et al., 2017), gas sensor (Lyson-Sypien et al., 2015), photocatalyst (Wen et al., 2015), and solar cell (Bai et al., 2014). Nanowire structure can enhance the performance of TiO_2 for those applications. It can provide larger surface area for adsorption species, increase the sensitivity for detecting gases, increase quantum yields for pollutant degradation, and improve charge transportation in solar cell.

There are two general approaches in the synthesis of nanomaterials and the fabrication of nanostructures; (i) top-down, and (ii) bottom-up. Top-down method refers to the fabrication of nanomaterials by reducing bulk material from ‘’big’’ size to ‘’nano’’ size, while bottom-up method corresponds to built nanomaterials from “small” components to more complex assemblies. Various techniques have been reported to synthesis nanostructured materials specially TiO_2 nanowires such as hydrothermal (Liu et al., 2016a), sol-gel (Miao et al., 2002), thermal evaporation (Wu et al., 2005b), chemical vapour deposition (Pradhan et al., 2003), and thermal oxidation (Lee, 2014). In this work, thermal oxidation with catalyst was selected due to its facility, and effectiveness.

2.4 Synthesis of TiO_2 nanowires by thermal oxidation

There are several published reports on the synthesis of TiO_2 nanowires by thermal oxidation with variation of synthesis routes which can be grouped into four: 1) thermal oxidation in air, 2) thermal oxidation in water vapour, 3) thermal oxidation in ethanol or acetone, 4) thermal oxidation with catalyst. All of these methods resulted in TiO_2 with nanowire structure. The comparison among them can be seen in Table 2.2.

Table 2. 2 Summary of synthesis TiO_2 nanowires by thermal oxidation work

Reference	Substrate	Temp. (°C)	Time (hr.)	Oxidant	Post annealing	Catalyst	Remarks
(Lee et al., 2010)	Commercially pure Ti plates	600	8	oxygen	-	-	
(Lee, 2016)	TiO powder	1000	2	Air	-	-	
(Motte et al., 1976)	Commercially pure Ti plates	650	120	Water vapour	-	-	
(Peng et al., 2005)	Commercially pure Ti plates	850	1.5	Water vapour	-	-	
(Peng and Chen, 2004)	Commercially pure Ti plates	850	1.5	mix. argon-acetone	-	-	Nanowire coated with carbon
(Daothong et al., 2007)	Commercially pure Ti wires	750	3	Ethanol vapour	450 °C; 2 hours; in air	-	Anatase and rutile phases present
(Huo et al., 2009)	Commercially pure Ti foils	800	1	mix. argon-acetone	650 °C; 30 min. ; in air	-	Only rutile phase present
(Cheung et al., 2007)	Commercially pure Ti foils	650	2	Water vapour	-	KF	Rutile and K-Ti-O phase present

2.4.1 Thermal oxidation in air

Lee et al in 2010 reported that nanowire structure can grow on pure α-phase titanium substrate under limited supply of oxygen gas (Lee et al., 2010) (Figure 2.6 (a)). They oxidized pure α-titanium at 600 °C for 8 hours in a mix. of argon-oxygen gas at flowrate of 200 mL/min to obtain nanowire stucture. However, the nanowires formed were considered very short and thin with low areal density. In addition, oxidation duration was rather long.

A different method was reported by Lee in 2016 (Lee, 2016). Whereby TiO powders were oxidised in air at atmospheric pressure to gain TiO_2 nanowhisker structure (Figure 2.6 (b)). The nanowhiskers grew on the grain surface in adequate uniformity. Nevertheless, it needed high temperature (1,000 °C) for 2 hours in the oxidation process.

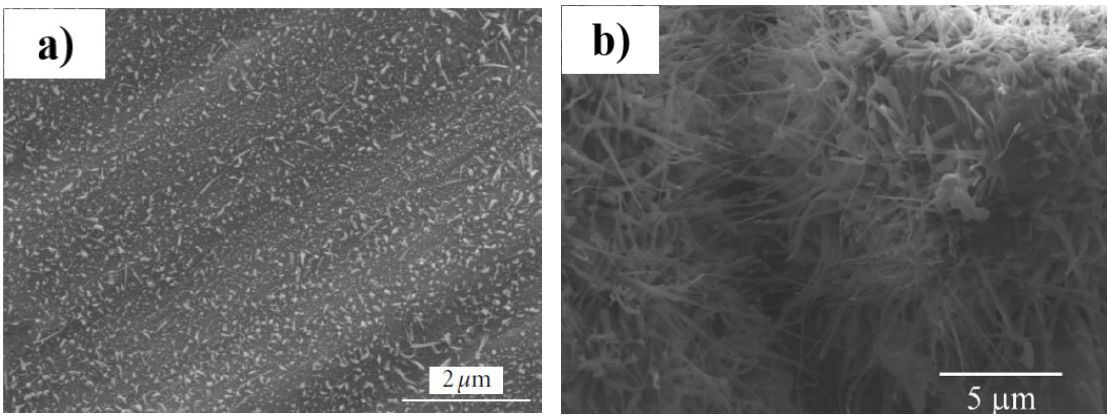

Figure 2. 6 a) SEM image of oxidized pure α-titanium at 600 °C for 8 hours in mix. Ar-O_2 gas (Lee et al., 2010), b) SEM image of oxidized TiO powder at 1000 °C for 2 hours in air (Lee, 2016)

2.4.2 Thermal oxidation in water vapour

In 1975, Motte et al discovered the formation of TiO_2 whiskers by oxidising pure titanium at 650 °C for 120 hours in the presence water vapour (P_{H2O} = 1.63 Torr). This could be the earliest report on TiO_2 whiskers fabricated by thermal oxidation in water vapour. The